4. Numerical Simulation

In the following we present some results from numerical model calculations which use the measured ground surface temperature variations *T(t)* at the *Beiluhe* test embankment as input data. The model was set up with the commercial finite element software *COMSOL Multiphysics*, Version 4.2. It is two-dimensional, i.e. the domain of computation is a vertical cross section, with x being the lateral coordinate (across the embankment) and y being the vertical coordinate. Dimensions and layering of the embankment and the natural ground have been chosen similar to those used in previous papers by [Lai et al. 2004] and [Lai et al. 2006]. The extension of the computational domain in lateral direction is 30 m in both directions from the road center, and the depth extension is 30 m from the natural surface. The total road width is 8 m and the embankment slopes have an inclination of 33°. The total height of the embankment above ground level is 4 m. The natural ground is assumed to consist of three layers with different thermo-physical properties: (i) a 2 m thick surface layer composed of clay with moderate water content, (ii) a 3 m thick ice-rich clay layer, and (iii) a bottom layer composed of metamorphic rock with low water content. The embankment material is assumed to consist of a mix of gravel and grit with low water content. Water content and thermo-physical parameters of the different layers in frozen and unfrozen condition are listed in Table 1. For the density, which is necessary to calculate the volumetric heat capacity from the given heat capacity by weight, a value of 1800 kgm^{-3} was used throughout. In addition the melting heat of ice Q_{melt} = 3.33 ×10^5 Jkg^{-3} is needed to run the model.

Table 1: Thermo-physical parameters of the materials used in the numerical simulation. The index f refers to the frozen state, the index u to the unfrozen state. k, C and w_c are the thermal conductivity, the heat capacity per unit mass, and the water content.

Material	k_f [Wm^{-1}K^{-1}]	C_f [Jkg^{-1}K^{-1}]	k_u [Wm^{-1}K^{-1}]	C_u [Jkg^{-1}K^{-1}]	w_c [%]
gravel&grit	1.98	1063	1.919	1237	3.4
clay	1.351	1309	1.125	1044	10.0
ice-rich clay	1.580	728	1.130	839	50.0
metamorphic rock	1.824	1026	1.474	1166	6.3

Next initial and boundary conditions have to be defined. As a starting condition for the calculation the complete domain including the embankment is frozen at constant temperature of -3°C, which is a typical temperature of the deep permafrost around the *Beiluhe* region (although rather on the lower limit of the profiles measured in boreholes). This constant low temperature is also used as the bottom boundary condition of the computational domain. At the two side boundaries a zero heat flux condition is adopted. The surface boundary consists of various parts, where temperature varies in different ways depending on the awning protection of the side slopes, according to formula (1) given in the previous section. A is the yearly averaged embankment slope surface temperature and B is the amplitude of the temperature variation around this average over one year. These coefficients are different depending on the presence or absence of the awning measure. On the natural ground to the left and right of the embankment and on the road surface values as given in [Lai et al. 2004] are used. In Table 2 the values of the coefficients A and B are listed.

Table 2: Coefficients A and B for the temperature variations at the different parts of the surface.

Surface	A[°C]	B[°C]
Natural ground	-0.40	+12.00
Road surface	+2.60	+15.00
Embankment slope with awning	-1.15	+7.72
Embankment slope without awning	+1.96	+10.79

To include climatic warming into the simulation, Eq. (1) for the ground surface temperature $T(t)$ must be extended by an additional term, resulting in the expression

$$T(t) = A + B \sin(2 \pi t/D + \pi/2) + C (t - t_a)/(t_e - t_a) \quad (2)$$

with C being the temperature rise caused by global warming within the simulated time period. This temperature rise is assumed to be linear in time, thus C is also a constant coefficient in the simulation. In all the simulations presented below $(t_e - t_a)$ = 50 years was used. In order to study the influence of climatic warming on the variation of the melting/freezing depth, the climate warming parameter was varied as C = 0 K, 1 K, 2 K, 3 K.

First, Figures 4 and 5 show the evolution of the temperature field and the melting/freezing isotherm over a period of two years, for the case C = 0 K, i.e. without climatic warming. In these runs the simulation was done over 50 years, following the solution from week to week. The figures show the typical evolution of the temperature field (color plot) and the melting isotherm (white contour) over a period of two years, in steps of three months. Figure 4 shows the case without any awning protection, while in Figure 5 both side slopes are protected by the awning measure. The sequence begins in early July, when the radiation is strongest and the melting/freezing line should be at the deepest level. The influence of the awning measure can be directly seen by comparing the corresponding panels in the two figures, because they represent the same point in time.

One interesting feature that is found from these simulations is that the temperature pattern and the profile of the melting/freezing line do not repeat every year in the same way. In some years the soil does not fully freeze in winter time. Instead, there is a closed region below the road where the soil remains unfrozen. However, there are also years where the whole domain becomes frozen in winter time. Moreover, when making a video from the simulations with a one week resolution observing the motion of the melting/freezing front, one can recognize that sometimes there exist two melting/freezing fronts which merge in the course of the evolution and sometimes disappear completely at wintertime. This behavior is associated with the thermal properties of the soil layers and with the thermal skin depth. There is a superposition of the forced temperature variation caused by the seasonal surface temperature change on the one hand and the inward motion of the heating and cooling waves, which depends on the thermal parameters of the soil layers and on the heat release and consumption caused by melting and freezing processes.

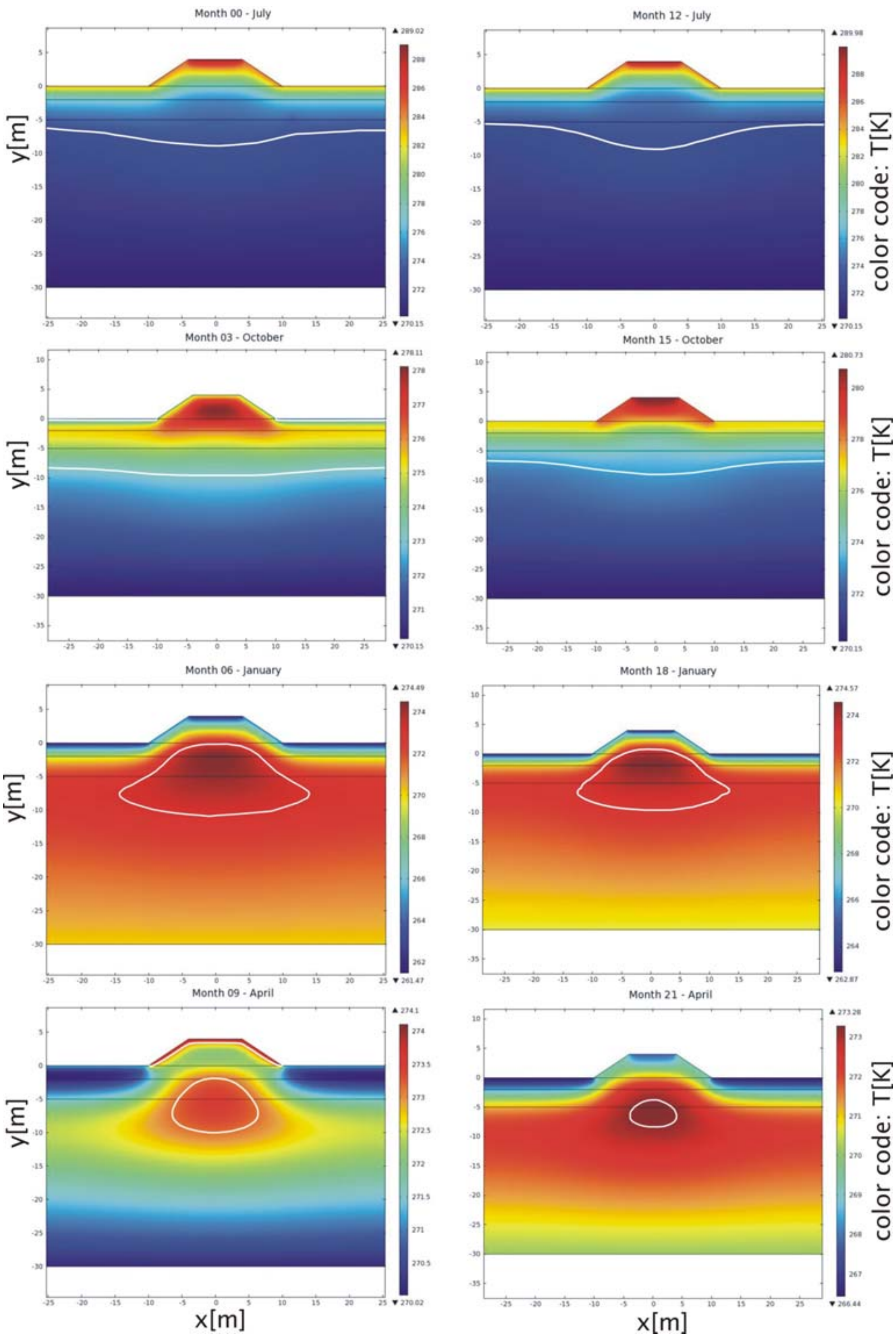

Figure 4: Temperature field variation and melting/freezing isotherm (white line) for a two years period (year 15 – year 17) in a numerical simulation performed over 50 years. In this simulation it is assumed that there is no awning protection.

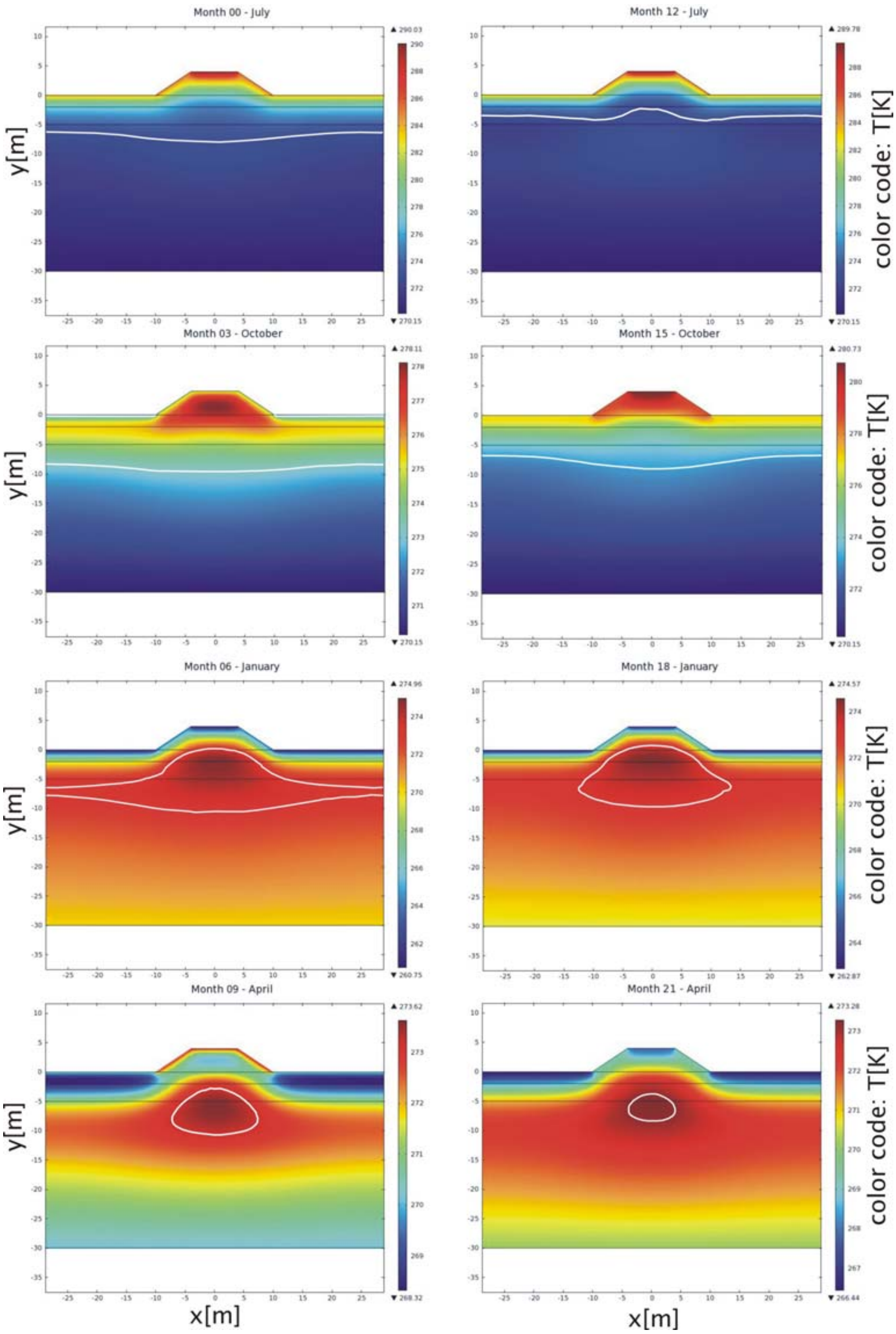

Figure 5: Temperature field variation and melting/freezing isotherm (white line) for a two years period (year 15 – year 17) in a numerical simulation performed over 50 years. In this simulation it is assumed that both slopes are protected by the awning measure.

Figure 6 illustrates the influence of the climatic warming trend. It shows the frost depth with and without awning measure at the time of strongest solar irradiation (end June/begin July) and compares the profiles of the melting isotherm with and without the awning measure. As can be seen by comparing the red full and the blue dotted lines, The summer melting level under road and embankment leads to a more shallow melting and thus to a better protection of the permafrost. In the nominal case without climatic warming the summer melting line is around 6 m below the natural ground and under the road it is almost 8 m below ground level without awning measure, but only 3 m when the awning measure is applied. For the expected climatic warming trend of 2 K within 50 years the summer melting line goes down to 12 m below natural ground, but there is still a clear difference between awning and no awning case. For the more extreme case of 3 K per 50 years the overall summer melting depth increases to more than 15 m, but there is no longer a big difference between awning and no awning case.

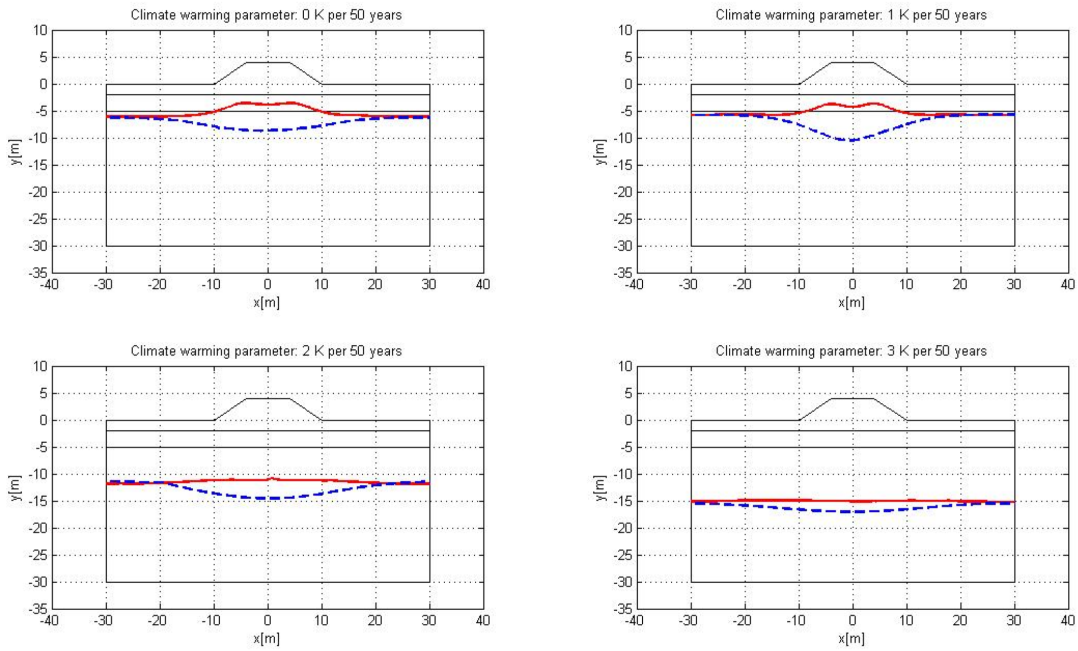

Figure 6: Influence of the awning measure (assumed to be implemented on both side slopes) on the position of the melting/freezing front in midsummer (i.e. when the net irradiation is at its maximum). Red full lines: *with awning*; blue dotted lines: *without awning*.

5. Summary

In this paper we have presented new measurement results on the seasonal variation of the ground surface temperature and net irradiation on the slopes of a test embankment situated on the Tibetan High Plateau near the *Beiluhe* Research Station in 4500 m height above sea level. Data were taken over a period of more than a year to cover a complete seasonal variation of ground temperature and net radiation. Measurements were done in parallel at two positions along the embankment slope: (i) at a position facing free sky and (ii) at a position shaded from solar radiation by an awning board. In order to study the effectiveness of the awning for the protection of the underground permafrost, numerical simulations over a reasonably long time period were made, using the measured surface temperature data as boundary conditions. The results show that in the long term the awning protection has a clear effect on the melting depth of the ice during summer time. Moreover, to some extent it is also able to counter the disastrous effect of the global climate warming, which is particularly severe on the Qinghai-Tibet Plateau, because of the higher solar irradiation due to its high altitude. In conclusion, the results of our measurements in conjunction with the numerical simulations indicate that in the high altitude regions awning measures along the embankments can significantly help to protect the permafrost.

ACKNOWLEDGEMENTS
This project was supported by the Funds of the State Key Laboratory of Frozen Soils Engineering, CAS (Grant No. SKLFSE-ZY-03), the Program for Innovative Research Group of Natural Science Foundation of China (No. 41121061), the National Key Basic Research Program of China (973 Program)(No. 2012CB026106), the Project for Excellent State Key of Natural Science Foundation of China (No. 41023003) and the National Natural Science Foundation of China (Grant Nos. 50976120, 41001041).

REFERENCES

Cheng Guodong (2003): The Impact of local factors on permafrost distribution and its inspiring for design Qinghai-Xizang railway. *Science in China (Series D)* 33 (6), 602-607.

Feng Wenjie, Ma Wei, Li Dongqing, Zhang Luxin, (2006): Application investigation of awning to roadway engineering on Qinghai-Tibet plateau. *Cold Regions Science and Technology* 45, 51-58.

Feng Wenjie, Wen Zhi, Sun Zhizhong, Wu Junjie (2009a): Application and effect analysis of the awning measure on cold regions - Recent development of research on permafrost engineering and cold region environment. *Proceedings of the Eighth International Symposiun on Permafrost Engineering*, 15-17 October, Xi'an, China, 148-153.

Feng Wenjie, Ma Wei, Niu Yonghong, (2009b): Simulate analysis of the wind speed variation under the awning. *Journal of Glaciology and Geocryology* 31(1), 106-112.

Feng Wenjie, Koemle N.I., Niu Yonghong, Sun Zhizhong, Li Guoyu, Yu Wenbing (2011): Numerical analysis of wind speed variation under awning boards covering embankment side slopes. *Cold Regions Science and Technology* 68, 162-172.

Feng Wenjie, Ma Wei, Sun Zhizhong, Li Guoyu, Yu Wenbing, Zheng Jianfeng (2011): Radiation effect analysis of the awning measure on the embankment slope field test in cold regions permafrost engineering. *Proceedings of the IX. International Symposium on Permafrost Engineering*, 3-7 September 2011, Mirny, Russia, pp. 319-325.

Gong Yuanfa, Duan Tingyang, Chen Longxun, et al. (1997): Outline of observational study of Sino-Japan Cooperative Program on Asian monsoon over Tibetan plateau. *Journal of Chengdu Institute of Meteorology*, 1997 (1), pp. 18-27.

Hu Zeyong, Qian Zeyu, Cheng Guodong, Wang Jieming (2002): Influence of solar radiation on embankment surface thermal regime of the Qinghai-Xizang railway. *Journal of Glaciology and Geocryology* 24(2), 121-128.

Hu Zeyong, Cheng Guodong, Gu Lianglei et al. (2006): Calculating method of global radiation and temperature on the roadbed surface of Qinghai-Xizang railway. *Advances in Earth Science* 21(12), 1304-1313.

Jin Huijun, Li Shuxu, et al. (2000a): Permafrost and climatic change in China. *Global and Planetary Change* 26, 387-404.

Jin Huijun, Li Shuxun, et al. (2000b): Impacts of Climatic Change on Permafrost and Cold Regions Environments in China. *Acta Geographica Sinica* 55(2),161-173.

Kondratjev V.G. (1996): Strengthening railroad bass constructed on icy permafrost soil. *Proceedings of the Eighth International Conference on Cold Region Engineering*, Fairbanks, Alaska, August 1996, 688-699.

Lai Yuanming, Wang Qiusheng, Niu Fujun, Zhang Kehua (2004): Three-dimensional nonlinear analysis for temperature characteristic of ventilated embankment in permafrost regions. *Cold Regions Science and Technology* 38, 165-184.

Lai Yuanming, Zhang Mingyi, Liu Zhiqiang, Yu Wenbing (2006): Numerical analysis for cooling effect of open boundary ripped-rock embankment on Qinghai-Tibetan railway. *Science in China: Series D Earth Sciences* 49(7), 764-772

Ma Wei, Cheng Guodong, Wu Qingbai (2002): Preliminary study on technology of cooling foundation in permafrost regions. *Journal of Glaciology and Geocryology* 24(5):579-587.

Koemle N.I., Feng Wenjie (2009): Variation of the frost boundary below road and railway embankments in permafrost regions in response to solar irradiation and winds. *Proceedings of COMSOL Conference* 2009, Milan, Italy, October 14-16.

Shi Lei, Li Ning, Li Guoyu, Bi Guiquan (2007): Stability analysis of the awning in road engineering in permafrost regions. *Journal of Glaciology and Geocryology* 29(6), 986-991.

Zhang Luxin, Yuan Sicheng, Yang Yongping (2003): Mechanism and prevention of deformation cracks of embankments in the permafrost region along Qinghai-Xizang railway. *Quaternary Sciences* 23(6), 604-610.

Numerical re-analysis of natural heat convection tests to assess the intrinsic permeability of rock-fill

Dhyser Y., Côté J., Lebeau M. & Konrad J.M.
Civil Engineering Department, Laval University, Quebec, Canada

ABSTRACT: Generally, heat transfer in soils is governed by conduction. In rock-fill materials, however, the pore sizes are large enough to promote heat convection from the motion of air under pressure gradient (forced convection) or temperature gradient (natural convection). It has been found that convection significantly influences the heat transfer in rock-fill embankments such as railways, roadways and embankment dam in cold regions. The material characteristics that influence the most the rate of convection heat transfer is the intrinsic permeability.

In a previous study, Côté et al. (2011*a*) developed a heat transfer cell where natural convection conditions were applied to 1 m^3 rock-fill samples in order to establish their intrinsic permeability. They analysed the experimental data using an analytical relationship between the Nusselt number (Nu) and the Rayleigh number (Ra). This theoretical relationship is valid for perfectly insulated and impervious 2-dimensional square enclosure. As shown by the deviation from intrinsic permeability models for porous materials, the use of the theoretical relationship as induces a bias in the experimental intrinsic permeability values.

In this paper, the heat transfer within the actual experimental heat transfer cell is analysed using numerical modelling of natural convection allowing to account for heat transfer in and out the imperfectly insulated cubic cell. A new Nu-Ra relationship is developed for this experimental setup. The previous experimental data are re-analysed according this Nu-Ra relationship in order to establish more accurate intrinsic permeability for values for the studied rock-fill materials. The results are compared to existing permeability models.

KEYWORDS: Porous media, natural convection, finite elements, numerical modelling, intrinsic permeability.

1. INTRODUCTION

Heat transfer in soils is generally governed by conduction. However, depending on the soil or geomaterial characteristics, other heat transfer mechanisms may be involved. Johansen (1975) established the domains of predominance of each type of heat transfer as a function of effective particle diameter (d_{10}) and degree of saturation (Sr). Heat convection was found to be the main heat transfer mechanism in gravels and coarser materials, especially in rock-fill materials used in embankment construction (Goering and Kumar, 1996; Lebeau and Konrad, 2007 and 2009).

Natural convection occurs in rock-fill embankment when the temperature at the surface becomes lower than that at the bottom. Air motion is initiated due to density gradients: the warm and lighter fluid at the bottom flows upward while the cool and heavier fluid at the top flows downward. The typical circular motion results in an increased heat transfer rate compared to pure conduction found under similar gradient (cool bottom, warm top).

The material characteristic that influences natural convection is the intrinsic permeability (m^2). Côté et al. (2011*a*) used the analytical solution to convection heat transfer from Schubert and Strauss (1979) to establish the intrinsic permeability from experimental heat transfer tests. This solution was obtained for a perfectly insulated square enclosure. As the experimental cell used in the Côté et al. (2011*a*) study is not perfectly insulated, the heat transfer rates for a given thermal gradient may differ from that predicted by the analytical solution of Schubert and Strauss (1979). In order to improve the assessment of the intrinsic permeability, a suitable numerical solution taking into account the characteristics of the test cell needs to be developed.

The objectives of this paper are to: (i) present the numerical model of the heat transfer (and especially natural convection) inside the cell test, (ii) develop a numerical solution to the convection heat transfer occurring in the experimental test cell and (iii) re-analyse the results obtained by Côté et al. (2011*a*) and propose improved intrinsic permeability values for rock-fill materials.

2. STUDY CONTEXT

Numerical studies have been carried out to model the natural convection in porous media. Goering and Kumar (1995) have studied road embankments in cold climates to assess the impact of permeability on the ground temperature and on the thermal equilibrium of permafrost. Thawing of permafrost due to road construction is a major problem in cold regions. It was shown the high permeability of embankment materials promotes higher heat extraction rates and may ultimately prevent the frozen ground from thawing.

Another interesting study was carried out by Lebeau and Konrad (2007, 2009) to verify the assumption made by Konrad (Konrad et al., 2006) on the potential effect of natural convection on the freeze of the toe drain of a rock-fill embankment. It was shown that if permeability of the rock-fill was set to 5.10^{-7} m^2, convection could take place and lead to the freezing of the toe drain even if the dam is located in a non permafrost area.

The challenge was then to assess the actual intrinsic permeability of rock-fill materials. The preliminary study by Côté et al. (2011*a*) showed that the intrinsic permeability could be assessed using natural convection testing. Four cobble materials with d_{10} ranging from 0.092 m to 0.15 m were tested and analysed using the Schubert and Straus (1979) solution. The results are summarized in table 1:

Table 1. Experimental results of heat convection tests (Côté et al., 2011*a*; Fillion et al., 2011). Note: $\mathbf{d_{10}}$: effective particle diameter; **n**: porosity; $\boldsymbol{\lambda_{eq}}$: overall thermal conductivity; **K**: permeability.

materials #	$\mathbf{d_{10}}$ m	**n**	$\boldsymbol{\lambda_{eq}}$ W/mK	**K** 10^{-6} m^2
1	0.15	0.41	1.02	3.9
2	0.13	0.41	0.95	2.1
3	0.092	0.39	0.71	1.5
4	0.100	0.37	0.83	2.9

3. NUMERICAL MODEL

To develop the numerical model, we consider a fluid (e.g. the air) moving inside a porous medium (e.g. the rock-fill). Natural convection is a very complex phenomenon because it depends on many characteristics of the materials (the fluid and the porous media). In order to model it and to obtain an efficient code, several assumptions were made.

The first is to neglect the moisture content of the fluid. It is considered dry and thus composed of a single phase. It is also considered incompressible. Then the porous media is considered homogeneous and isotropic since the porous media is formed with small blocks hand-placed in the test cell, block by block with particular care for homogeneity. Also, local thermal equilibrium is considered, so in all points of the interface between the fluid and the porous medium, the temperature (T) of the fluid equals the one of the porous medium and only the fluid density depends on temperature. All the others characteristics of the fluid and of the porous media are constant. Finally, it is considered that Darcy's Law is valid and that the test cell walls are impervious. The numerical model is based on two of the equations of Navier-Stockes: the conservation of the mass and the conservation of the energy.

Assuming steady-state and the previous assumptions, these equations are, respectively (Nield and Bejan, 1999):

$$\vec{\boldsymbol{\nabla}}.\vec{\boldsymbol{v}} = 0 \qquad [1]$$

$$\lambda_{eq}.\nabla^2 T = \left(\rho.c_p\right)_f.\vec{\boldsymbol{v}}.\vec{\boldsymbol{\nabla}}T \qquad [2]$$

where $\vec{\boldsymbol{v}}$ and T are Darcy's velocity and temperature; c_p, ρ and λ_{eq} represent respectively the specific heat capacity of the fluid, the density of the fluid (function of the temperature) and the overall thermal conductivity.